Journal of Colloid and Interface Science 578 (2020) 77–88

Contents lists available at ScienceDirect

Journal of Colloid and Interface Science

journal homepage: www.elsevier.com/locate/jcis

Pore opening and breathing transitions in metal-organic frameworks: Coupling adsorption and deformation

Filip Formalik [a,b,*], Alexander V. Neimark [c], Justyna Rogacka [a], Lucyna Firlej [a,d], Bogdan Kuchta [a,e]

[a] Department of Micro, Nano and Bioprocess Engineering, Faculty of Chemistry, Wroclaw University of Science and Technology, Wroclaw, Poland
[b] Department of Theoretical Physics, Faculty of Fundamental Problems of Technology, Wroclaw University of Science and Technology, Wroclaw, Poland
[c] Department of Chemical and Biochemical Engineering, Rutgers, The State University of New Jersey, Piscataway, NJ, USA
[d] Charles Coulomb Laboratory, University of Montpellier, CNRS, Montpellier, France
[e] MADIREL, Aix-Marseille University, CNRS, Marseille, France

GRAPHICAL ABSTRACT

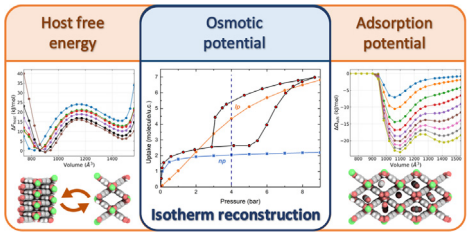

ARTICLE INFO

Article history:
Received 4 April 2020
Revised 27 May 2020
Accepted 28 May 2020
Available online 1 June 2020

Keywords:
Phase transformations
Metal-organic framework
Osmotic potential

ABSTRACT

Soft porous crystals undergo large structural transformations under a variety of physical stimuli. Breathing-like transformations, occurring with a large volume change, have been associated with an existence of bi-stable or multi-stable crystal structures. Understanding of the mechanism of these transformations is essential for their potential applications in gas adsorption, separation and storage. However, the generic description is still missing. Here, we provide a detailed, multiscale qualitative and quantitative analysis of the adsorption-induced "breathing" transformations in two metal organic frameworks (MOFs): MIL-53(Al) which is a reference case of our approach, and recently synthesized JUK-8, which does not show any bistability without adsorbate. The proposed approach is based on atomistic simulations and does not require any empirical or adjustable parameters. It allows for a prediction of potential structural transformations in MOFs including the adsorption induced deformations derived from adsorption stress model. We also show that the quantitative agreement between calculated and experimental results critically depends on the quality of the dispersion energy correction. Our methodology represents a new, powerful tool for designing and screening of flexible materials, alternative and complimentary to experimental approaches.

1. Introduction

Flexible metal-organic frameworks (MOFs) have recently became subject of intense research due to their unprecedented ability to undergo various structural transformations [1–4], such as breathing (observed in MIL-53-type materials) [5–8], gate opening (e.g. ZIF-8) [9] and negative gas adsorption, NGA (DUT-49) [2].

* Corresponding author at: Department of Micro, Nano and Bioprocess Engineering, Faculty of Chemistry, Wroclaw University of Science and Technology, Wroclaw, Poland.
E-mail address: filip.formalik@pwr.edu.pl (F. Formalik).

https://doi.org/10.1016/j.jcis.2020.05.105
0021-9797/

The structural transformations in MOFs may be induced by different stimuli: external pressure (ZIF-8 [9], MIL-53(Cr) [10]), temperature (MIL-53(Al) [11], MIL-53(Ga) [12]), electric field (MIL-53(Cr) [13]), and gas adsorption (ZIF-8 [9], MIL-53(Al) [14], DUT-49 [2]). Gas adsorption may induce not only framework expansion but also its contraction which - in the case of NGA - causes expulsion of the adsorbed gas [2]. A large spectrum of statistical-mechanical and numerical methods has been used in the past to understand the mechanisms of structural transformation of MOFs. Here, we present a multiscale computational approach to account simultaneously for adsorption and deformation in two flexible structures: (i) MIL-53(Al) which exhibits breathing transformation between narrow pore (*np*) and large pore (*lp*) phases [6], and (ii) a recently synthesized JUK-8 structure [15] that shows pore-opening transformation between closed pore (*cp*) and open pore (*op*) phases accompanied by a significant volume change.

The breathing transitions were first observed in MIL-53-type materials with inorganic centers containing Al, Cr, Sc, Fe, Ga and In [6,7,12,16–18]. The first attempt to explain breathing mechanism in MIL-53(Al) was given by Ramsahye *et al.* [19] while interpreting the simulated isotherms of CO_2 adsorption in rigid *np* and *lp* structures of MIL-53(Al), determined by XRD. The authors assigned the experimentally observed step on the isotherm at around 6 bars to *np-lp* transition. Stability of the *np* structure was attributed mainly to electrostatic interactions of CO_2 quadrupole with polar hydroxyl groups of inorganic chains, preventing the pore from opening at low adsorption pressure. The same breathing mechanism has been also deduced from MD simulations of CO_2 adsorption in MIL-53(Cr) [20]. Similarly, during thermal desorption of water from MIL-53(Fe) Millange *et al.* [21] observed that the fully loaded low-temperature phase (MIL-53(Fe)*lt*) contains narrow pores, that progressively open upon desorption (an intermediate state, MIL-53(Fe)*int* contains pores of two different sizes: completely closed and slightly opened) before the transition into MIL-53(Fe)*ht* (high-temperature) phase with fully open pores. In combined experimental – simulation study Chen *et al.* [17] showed that MIL-53(Sc)*cp* (condensed pore) and MIL-53(Sc)*vnp* (very narrow pore) phases may co-exist upon removing of post-synthetic solvent and further heating up the structure. On the other hand, adsorption of CO_2 leads to structure transformation into MIL-53(Sc)*lp* phase with intermediate stage similar to one observed in MIL-53(Fe). Boutin *et al.* [22] showed that in the limited range of temperatures the *np-lp* transition in MIL-53(Al) occurs regardless the chemical nature or size of the adsorbate, if only the ratio of the Henry constants fulfill the condition $K_{np}/K_{lp} > 1$. Ghoufi *et al.* [23] suggested that in MIL-53(Cr) the transition from *lp* to *np* phase upon CO_2 adsorption is continuous, goes through the intermediate *int* phase, and is triggered by a *soft phonon*. Coudert *et al.* generalized the description of the breathing transformations in MOFs using the osmotic thermodynamic potential [24,25]. The authors analyzed adsorption of gases in a set of flexible MOFs (including MIL-53(Al)) and concluded that the mechanism of adsorption-induced transformation depends on the profiles of osmotic free energy in both phases. Two points at which the osmotic potentials of *np* and *lp* phases cross each other were associated to experimentally observed transitions as the gas pressure increases: from *lp* to *np* phase at low pressures (0.5 bar), and then from *np* to *lp* phase (5 bar). In further studies of xenon adsorption in MIL-53(Al), Neimark *et al.* [26] proposed an adsorption stress model explaining mechanism of transformation, and assumed that the structural transition occurs when the adsorption stress (the stress exerted by the guest molecules on the host matrix) exceeds the limiting (threshold) stress that the given phase can withhold. The threshold stress delimits then the region of elastic deformation and that of spontaneous plastic deformation that leads to a structural transformation of the framework. The adsorption stress model coherently explains the phase transformations in MIL-53(Cr) induced by both adsorption and external pressure [27]. The model was also applied to describe MIL-53(Al) framework deformations during CO_2 and CH_4 adsorption, and to explain the existence (CO_2) or the absence (CH_4) of steps on the isotherms during adsorption process [14,27]. Triguero et al. used a stochastic model and described the *np-lp* transition in MIL-53 as a nucleation-driven process, consisting in consecutive shearing of the layers of the unit cells [28,29]. Ghysels *et al.* [30] proposed a generic parametrization of the free energy and account for the free energy of both: the host-host and host-guest interactions. This approach allowed to create the energy landscapes for all configurations of deforming MIL-53(Cr) framework and gas chemical potentials, and provided the complete phase diagram for CH_4 and CO_2 adsorption in this system [30]. For MIL-53(Al, Ga) and MIL-53 (Al)-F (with fluorine-functionalized linker), the free energy landscapes were further modeled using the MD technique, and accounting for various external stimuli (mechanical pressure, temperature, and gas chemical potential) [31]. Recently, Hoffman *et al.* [32,33] used the phonon analysis to explain the transition in MIL-53(Al) by softening of the vibration modes. The authors found several low-frequency modes (linker rotation, trampoline-like motion, and backbone rotation) at the Γ-point of Brillouin zone, that might be related to the onset of structure transformation. However, none of them exhibited softening when approaching the np-cp transformation. The question whether the breathing transitions are related to the presence of soft mode remains still open.

The breathing transformation have been also observed and modeled in MOFs other than MIL-53 family. Li and Kaneko [34] synthesized and analyzed Cu-based flexible MOF stabilized by a network of hydrogen bonds. Upon adsorption of N_2, CO_2 or Ar, at so-called *gate-pressure* of fluid, hydrogen bonds start to break creating 1D micropores in a shape of channels accessible for guest molecules. Similar gate-opening behavior has been also observed by Chen *et al.* [35] in an interpenetrated framework of Zn-based MOF. The most subtle adsorption-induced gate-opening was observed in ZIF-8 [9], where the reorganization of the adsorbate inside the pore and rotation of the linkers simultaneously led to an increase of the pore-limiting diameter [9,36]. Several groups pointed out that this deformation of the framework is strongly related to low-frequency phonons [37–39].

The MOFs from DUT family exhibits another phenomenon resulting from coupling between adsorption and frameworks deformation: NGA. In DUT-49 buckling of the organic ligand upon applied stress leads to contraction of the framework [40]. Evans *et al.* [40] applied atomistic simulations (both quantum and classical) and the osmotic potential to show that the open pore DUT-49*op* structure is stable at ambient conditions but upon methane adsorption, as the number of adsorbed molecules increases, the stability of closed-pore *cp* phase increases, leading to decrease of transition barrier between *op* and *cp* structures. Surprisingly, the isorecticular MOF DUT-48 does not undergo adsorption-induced transition [41]. Using DFT and MD methods Krause *et al.* [41] showed that it is due to fact that the ligand in DUT-48 is shorter than in DUT-49, and much larger stress is required to bend it.

Recently synthesized JUK-8 (JUK – Jagiellonian University Krakow, Fig. 1) with complex structure build from eight interpenetrated subnetworks [15] constitutes another example of breathing MOF. This material exhibits pore-opening transformation upon adsorption of CO_2 and H_2O molecules. Contrary to MIL-53 for which the energy profile shows two well-defined minima even for pristine (empty) structure, only *cp* structure of empty JUK-8 is stable, and the pores open when the pressure of the adsorbed gas increases.

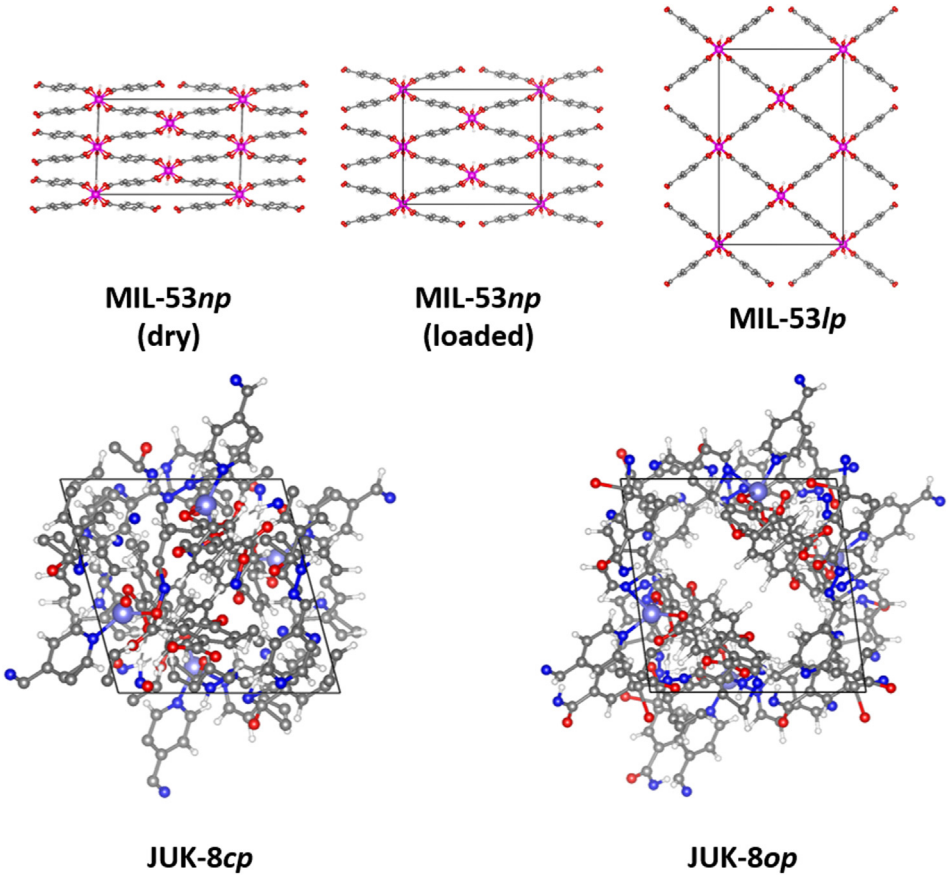

Fig. 1. Structures of MIL-53(Al) and JUK-8. The following notation was adopted over the whole paper: *np* - narrow pore, *lp* - large pore, *cp* - closed pore, *op* - open pore.

In the present paper we provide a comprehensive methodology for quantitative description of the phase transitions in flexible MOFs using the osmotic thermodynamic potential approach. The MOF and the adsorbate components of the osmotic potential are calculated for the whole range of unit cell volumes, respectively by fixed-volume DFT structures optimization and subsequent GCMC simulation of adsorption isotherms. From the landscape of the osmotic thermodynamic potential and the adsorption stress, we determine the adsorption isotherm and respective framework deformation during transformation. The proposed methodology is applied to interpret the structural transitions induced by CO_2 and CH_4 adsorption in MIL-53(Al), and by CO_2 adsorption in JUK-8 framework. The paper is organized as follows: in the section 2 we present the theoretical background and details on modelling techniques used for calculating the osmotic potential and adsorption stress. Section 3 describes the obtained results: free energy landscapes of host materials, calculated adsorption, and osmotic potentials, and then discusses the possibility of predicting *in-silico* adsorption isotherms and framework deformation in any flexible MOF materials. We also discuss the influence of rescaling the empirical dispersion correction of interaction models on the quality of quantitative results. The general conclusions are given in Section 4.

2. Theory and methodology

To characterize the structural transformations in MOFs we use the osmotic thermodynamic potential Ω_{os} [24] depending on the unit cell volume V, adsorbate chemical potential μ, external pressure P and temperature T:

$$\Omega_{os}(\mu, V, P, T) = G_{host}(V, P, T) + \Omega_{ads}(\mu, V, T). \tag{1}$$

Here the Gibbs free energy $G_{host}(V, P, T)$ decomposes as:

$$G_{host}(V, P, T) = F_{host}(V, T) + PV \tag{2}$$

$$F_{host}(V, T) = E_{el}(V) + F_{vib}(V, T) \tag{3}$$

where the electronic energy $E_{el}(V) = E_{DFT}(V) + E_{disp}(V)$ is a sum of the DFT-derived energy and empirical dispersion contribution describing long-range interactions. The vibrational contribution to free energy $F_{vib}(V, T)$ is calculated as:

$$F_{vib}(V, T) = \frac{1}{2}\sum_{i=1}^{3N} \hbar\omega_i(V) + k_b T \sum_{i=1}^{3N} \ln\left(1 - e^{-\frac{\hbar\omega_i(V)}{k_B T}}\right), \tag{4}$$

and depends on the frequencies ω_i of each mode ($N$is a number of atoms in the cell). The first term in Eq. (4) represents system zero-point energy (ZPE).

The second term in Eq. (1) is the grand thermodynamic potential of adsorbed phase:

$$\Omega_{ads}(\mu, V, T) = -RT \int_0^p \frac{N(p, V, T)}{p} dp, \tag{6}$$

where $N(p, V, T)$ is the adsorption isotherm calculated for a unit cell of given volume and temperature. Assuming the Langmuir model of adsorption, $N(p, V, T) = \frac{N_0(V,T)K_H(V,T)p}{N_0(V,T)+K_H(V,T)p}$, the Eq. (6) can be integrated analytically:

$$\Omega_{ads}(p, V, T) = -RTN_0(V, T) \ln\left(1 + \frac{K_H(V, T)p}{N_0(V, T)}\right). \tag{7}$$

The osmotic thermodynamic potential defined by Eqs. (1)–(6) implies two important approximations. Eq. (2) assumes that the external pressure is hydrostatic and the possible deviatoric stresses

are ignored. This assumption is realized in adsorption experiments with free standing samples (not exposed to any external stress), where the external pressure is equal to the bulk gas pressure. Eq. (6) assumes also that the adsorbate is an ideal gas.

By accounting for the vibrational and adsorption-related contributions to the total free energy, we were able to provide the full description of the systems deformations and phase transformations without any experiment-based adjustable parameters. In order to obtain volume-dependent landscapes of the osmotic potential, we prepared a set of framework structures in the range of unit cell volumes embracing the experimentally stable phases (from *np* to *lp* phase for MIL-53, from *cp* to *op* phase for JUK-8). For each volume of the unit cell the structure was optimized with DFT methodology using PAW method (as implemented in the VASP package [42–44]). The dispersion correction for long-range interactions was calculated applying the Grimme methods [45,46] as described in our previous papers [47] (D2 for MIL-53(Al), and D3 (BJ) for JUK-8). The convergence criteria are set to 10^{-6} eV for electronic degrees of freedom, and to10^{-3} eV/Å for ionic. Frequencies are calculated using the finite displacement method (with displacement of 0.01 Å). Eq. (4) was applied to calculate the vibrational free energy. Adsorption isotherms for CO_2, CH_4 adsorption in MIL-53, and CO_2 in JUK-8 were taken from our previous work [3,15].

The adsorption stress [48] exerted by adsorbed guest molecules on the host framework can be derived directly from the calculated adsorption isotherms. From the thermodynamic standpoint, the adsorption stress σ_a is defined as the derivative of the grand thermodynamic potential of the adsorbed phase $\Omega_{ads}(\mu, V, T)$ with respect to the cell volume V, at the given chemical potential μ of the adsorbate and the temperature T:

$$\sigma_a(\mu, T) = -\left(\frac{\partial \Omega_{ads}(\mu, V, T)}{\partial V}\right)_{\mu,T}. \tag{8}$$

If the Langmuir model is used to describe the adsorption isotherms, the adsorption stress can be calculated analytically:

$$\sigma_a = RT\left\{\frac{dN_0}{dV_c}\left[ln\left(1 - \frac{K_H p}{N_0}\right) - \left(\frac{K_H p/N_0}{N_0 + K_H p}\right)\right] + \frac{dK_H}{dV_c}\left(\frac{N_0 p}{N_0 + K_H p}\right)\right\}, \tag{9}$$

where K_H and N_0 are Henry constant and saturation capacity, respectively, and the derivatives $\frac{dN_0}{dV_c}$ and $\frac{dK_H}{dV_c}$ are calculated with respect to the cell volume V_c.

The volumetric strain ε of an isotropic sample in the elastic linear approximation is related to the framework volumetric modulus K and solvation pressure P_{sol} [48]:

$$\varepsilon = \frac{V - V_0}{V_0} = \frac{\sigma_a - P}{K} = \frac{P_{sol}}{K}, \tag{10}$$

The solvation pressure is defined as the difference between the adsorption stress and the bulk gas pressure: $P_{sol} = \sigma_a - P$. V_0 is the equilibrium volume of the dry sample, from which the strain is reckoned. The bulk modulus K can be estimated from the relation between the cell volume and the framework free energy: $K = V\frac{\partial^2 \Delta F_{host}}{\partial V^2}$ [33].

3. Results and discussion

3.1. Free energy landscapes of host frameworks

We start our analysis with the free energy landscapes of MIL-53 (Al) and JUK-9 calculated for the *dry* frameworks (without adsorbate, $P_{ext} = 0$). The landscapes $F_{host}(V, T)$, calculated at different temperatures, are presented on Fig. 2.

The double-well profiles in Fig. 2 (left panel) indicate the relative stability of *np* and *lp* phases of MIL-53(Al). For comparison, the potential energy of electronic interactions $E_{el}(V)$ is also shown. Clearly, the contribution of temperature-dependent vibrational free energy F_{vib} to the total free energy of the system is significant. It causes (i) a shift of the equilibrium *np* phase to a larger volume (by approx. 50 Å^3), and (ii) decrease of free energy difference between *np* and *lp* phases. When the temperature increases this effect becomes more pronounced. The calculated free energy difference for *np*-*lp* transition equals 12.7 kJ/mol, 10.0 kJ/mol and 5.8 kJ/mol for respectively 1 K, 200 K, and 500 K. However, the *lp* phase remains less stable than *np* phase over the whole range of temperatures, up to 500 K. This result disagrees with experimental observations [11]. A similar computational deficiency was already pointed out in Ref [33], and attributed to the neglection of anharmonicity of atoms' vibrations, and overestimation of the van der Waals interactions by the empirical corrections. We consider that the empirical parametrization of interaction parameters is the main source of the observed disagreement between computed and experimental data. In Section 3.5 we propose a solution to this problem which leads to the stabilization of *lp* phase at high temperatures.

Fig. 3 (left panel) shows the variation of optimized volumes of *np*, *lp* and *tp* (transient phase at the energy barrier) phases of MIL-53(Al) with temperature. The numerical results are in excellent agreement with experimental data [11] for *np* phase that exhibits a considerable thermal expansion with thermal expansion coefficient $\alpha_{MIL-53(Al)np} = 145 \cdot 10^{-6} \cdot K^{-1}$. For *lp* phase the volume of unit cell is only slightly overestimated (by 4%).

The free energy landscapes of JUK-8 (Fig. 2, right panel) shows only one minimum; it indicates that in the absence of external stimuli only one structure is stable at each temperature. The minimum shifts towards larger volumes with increase of the temperature from 3337 Å^3 at 1 K Å^3 at 1 K to 3485 Å^3 at 500 K. As in the case of MIL-53(Al), the vibrational contribution to the free energy is significant – electronic potential energy E_{el} has the minimum at a smaller cell volume (of 3290 Å^3). The unit cell expands when the temperature increases (Fig. 3, right panel), with thermal expansion coefficient $\alpha_{JUK-8cp} = 88 \cdot 10^{-6} \cdot K^{-1}$. The calculated volume agrees with the unique experimental value reported in [15].

3.2. Grand thermodynamic potential of adsorbed phase

Fig. 4 shows the adsorption isotherms simulated using GCMC in the generated MOF structures of different cell volumes (adsorption of CO_2 and CH_4 in MIL-53(Al) at T = 298 K and of CO_2 in JUK-8 at T = 195 K; for comparison, the experimental isotherms are also shown [3,14,15]. The isotherms were calculated starting from the cell volumes accessible for adsorbed molecules ($V > 970$Å^3 for CO_2 in MIL-53(Al), $V > 3180$Å^3 for CO_2 in JUK-8, and $V > 1060$Å^3 for CH_4 in MIL-53(Al)). It is clear that the experimentally observed isotherms of CO_2 adsorption cannot be associated to a single isotherm simulated assuming rigidity of the host framework, and that the abrupt increase of the adsorbed amount is a consequence of a structural transition within the adsorbent leading to a change of accessible volume. In the case of CH_4 adsorption in MIL-53(Al) both the experimental and calculated isotherm increase monotonically and does not show any features of phase transformations.

Fig. 5 shows the grand thermodynamic potential of adsorbed phaseΩ_{ads}, calculated according to the Eq. (6) by integration of the simulated isotherm at given cell volume. For MIL-53(Al), as the simulated isotherms are satisfactory approximated by the Langmuir model it is possible to perform analytical integration of isotherms (The details of Langmuir fitting are given in Supplementary Material,

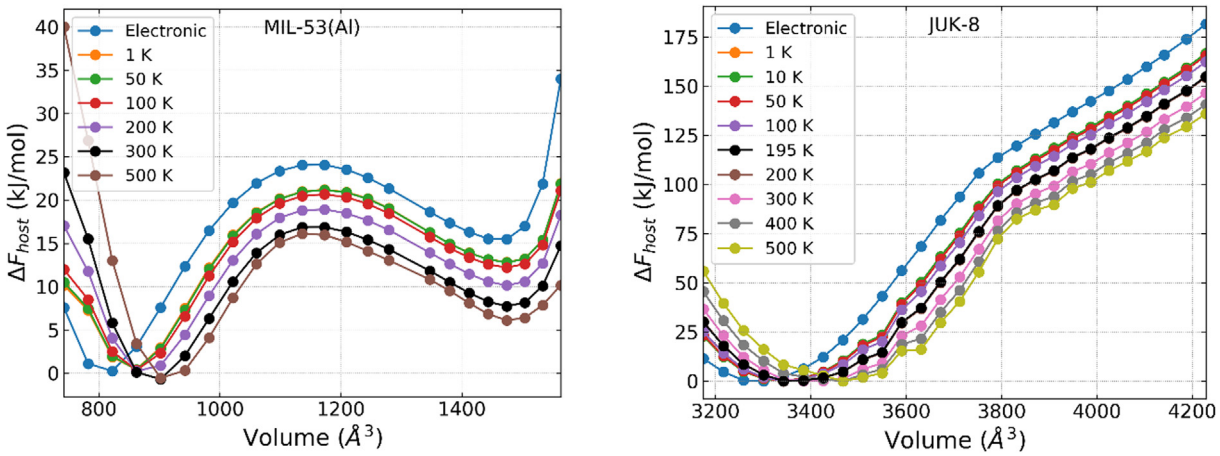

Fig. 2. Temperature dependence of the free energy landscapes for *dry* structures of MIL-53(Al) (left) and JUK-8 (right) in a function of unit cell volume. Profiles include electronic energy E_{el} and free energies F_{host}. The energy profiles are reckoned from the energy of *np* phase.

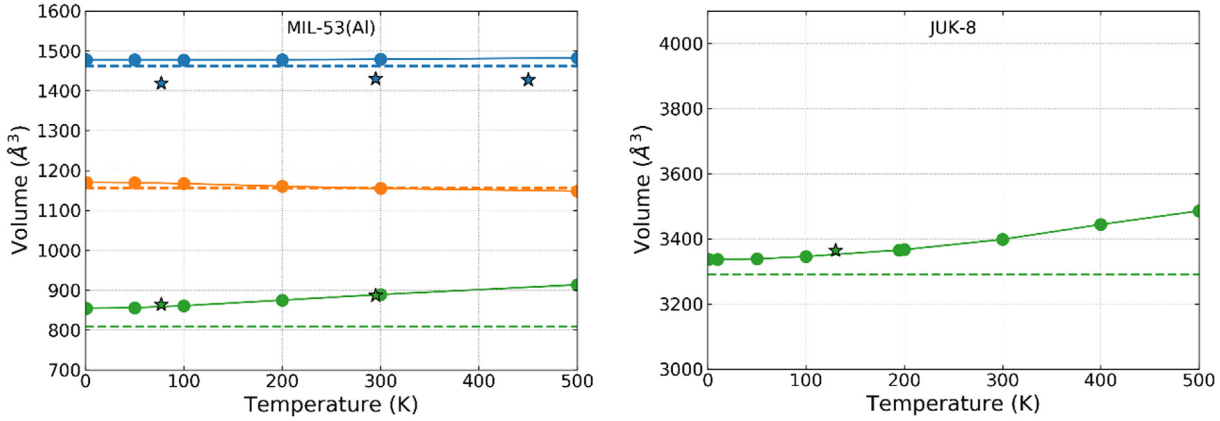

Fig. 3. Temperature dependence of the unit cell volumes for MIL-53(Al) (left panel) and JUK-8 (right panel). Dashed lines show the volumes of *np* and *lp* phases (and of unstable transient structure at the energy barrier) for which the electronic energy reaches minimum (maximum for transient structure). The stars represent XRD experimental data [11]. For MIL-53(Al), the green dots represent the volumes of the equilibrium np phase, the orange dots - unstable transient state at the energy barrier, the blue dots– equilibrium lp phase. For JUK-8, the green dots represent the equilibrium cell volume.

Fig. S1). For JUK-8, the calculated CO_2 isotherms could not be approximated by the Langmuir model and hence, to keep consistency the Ω_{ads} profiles were calculated by numerical integration of simulated isotherms for both MIL-53 and JUK-8.

For CO_2 adsorption in MIL-53(Al), at T = 298 K and pressures lower than 5 bar only one minimum of the Ω_{ads}potential exists and corresponds to the *np* phase. It appears at the volume of 1060 Å^3, roughly 100 Å^3 larger than the minimum observed for empty structure (Fig. 2, left panel). This difference results from the fact that pore in the empty *np* phase is too small to accommodate CO_2 molecules and needs to be first slightly expanded by the adsorbed gas. The absence of a second minimum in adsorption free energy profile is attributed to the strong electrostatic attraction between hydroxyl group of the MIL-53(Al) framework that balance the stress induced by (low) adsorption pressure. Therefore, at low pressure the CO_2 molecules play a role of *molecular clips* that prevent the structure from expanding.

At 5 bar, the second minimum on the Ω_{ads}potential emerges and becomes more and more pronounced when the gas pressure increases. It is related to the stabilization of the *lp* phase: as the *np* structure becomes fully filled by the adsorbed molecules, it is energetically more favorable for the framework to deform (undergoes structural phase transition from the *np* to the *lp* phase), and to absorb larger number of molecules.

The Ω_{ads}potential of CH_4 adsorption at 298 K in MIL-53(Al), at pressures lower or equal to 20 bar presents only one, very shallow minimum located at around 1450 Å^3. For higher gas pressures Ω_{ads}potential monotonically decreases with increasing volume. It suggests that in the *np* phase there are no specific (and strong) interactions between host framework and methane molecules; the adsorbed amount of gas is proportional to the accessible volume, and limited by the free energy of the material only; this aspect will be discussed further in the text.

The adsorption potential of CO_2 in JUK-8 for pressures lower than 0.05 bar shows only one, very shallow minimum (*cp* phase). When the gas pressure increases, a 2nd minimum appears. It suggests that, similarly as for CO_2 adsorption in MIL-53(Al), there exist some specific host-guest interactions that stabilize structures of smaller volumes. However, this minimum is much shallower than the minimum appearing at larger volume (-30 kJ/mol versus −188 kJ/mol).

3.3. Osmotic thermodynamic potential of the host-guest system

The equilibrium structures of MOF in the presence of adsorbed gas were determined by the minimization of the osmotic thermodynamic potential Ω_{os} (Equation (1)) that includes the host–host, guest–guest, and guest-host interactions. Fig. 6 presents the

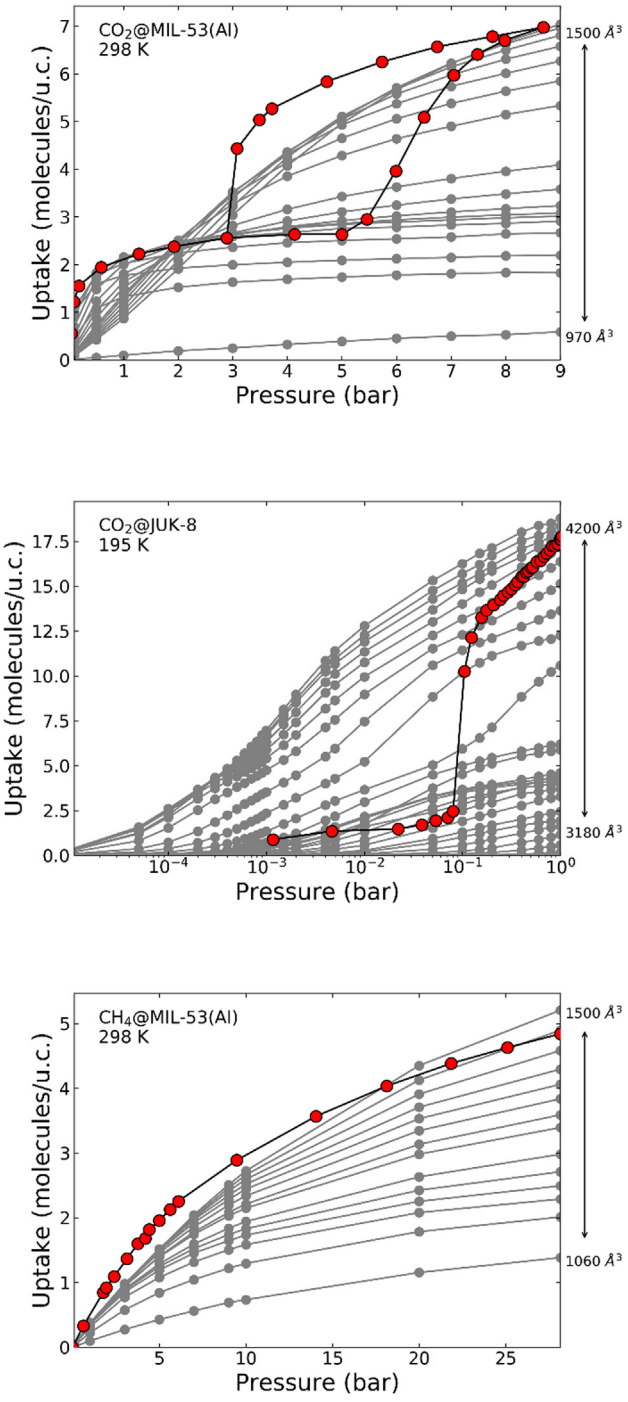

Fig. 4. Simulated adsorption isotherms of CO_2 in MIL-53(Al) (top), CO_2 in JUK-8 (middle) and CH_4 in MIL-53(Al) (bottom) [3,15]. Each isotherm was calculated at the fixed unit cell volume. The red points represent the experimental data [14,15].

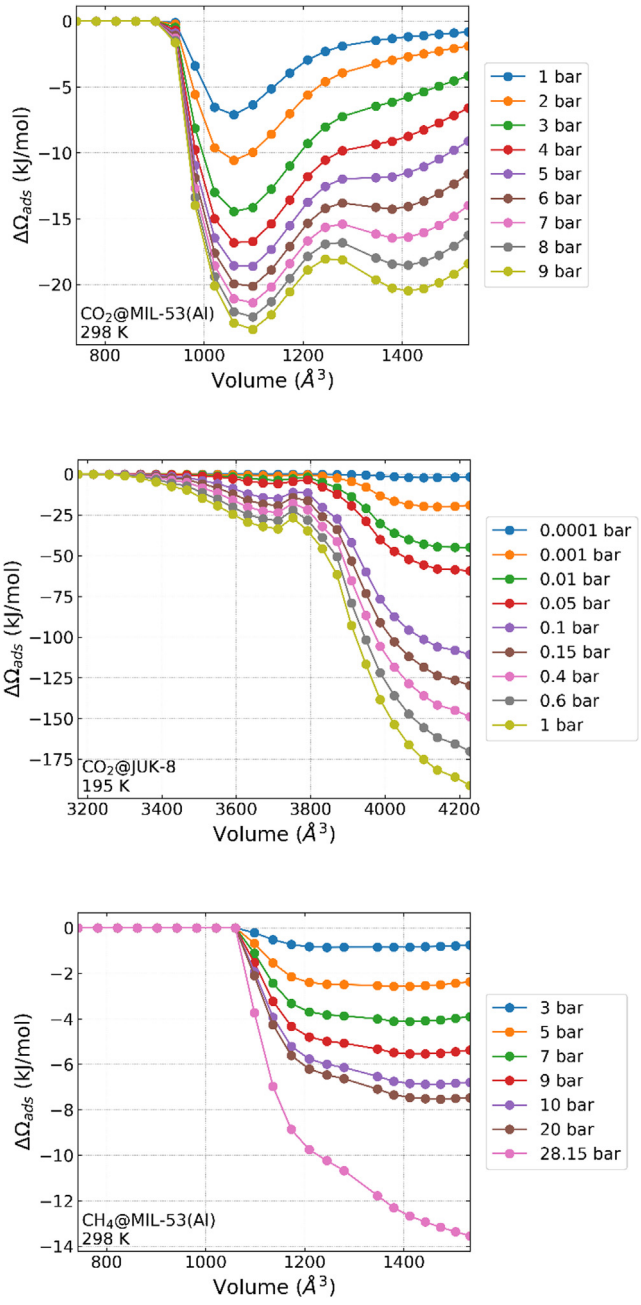

Fig. 5. Adsorption potential of CO_2 in MIL-53(Al) (298 K, top), CO_2 in JUK-8 (195 K, middle) and CH_4 in MIL-53(Al) (298 K, bottom). Full range of CO_2 gas pressures for JUK-8 is presented on Fig. S3.

osmotic potential landscapes for increasing gas pressures. In the case of CO_2 adsorption in MIL-53(Al) the two-well landscapes of Ω_{os} indicate the existence of two well defined *np* and *lp* phases. The *np* structure of 1021 Å^3 is more stable at pressures lower than 7 bar. For higher pressures, the osmotic potential minimum at 1474 Å^3 deepens, revealing the progressive stabilization of the *lp* phase. At the pressure of 7 bar both: *np* and *lp* phases are in equilibrium. When the pressure increases the second minimum, corresponding to *lp* phase, becomes deeper. The framework undergoes a structural (breathing) transition from *np* to *lp* phase, with a significant change of its volume. In experiments, the breathing transitions occur with a pronounced hysteresis (Fig. 4, top) due to a high energy barrier between the *np* and *lp* phases. The hysteresis occurs in the range of pressures between 3 bar and 6 bar, slightly below the equilibrium pressure of 7 bar predicted by our model. This difference is the most probably due the inaccuracies in the empirical correction of dispersion used in the calculations to account for the long-range van der Waals interactions in the system. This discrepancy can be avoided by adjusting the dispersion terms, which is discussed in paragraph 3.5.

The osmotic potential for methane adsorption in MIL-53(Al) does not indicate possibility of transition between *np* and *lp* phases upon adsorption. Adsorption may occur only in the structures of volume larger than 1060 Å^3, and only one minima of osmotic potential exists at 1460 Å^3; this value agrees with the experimental

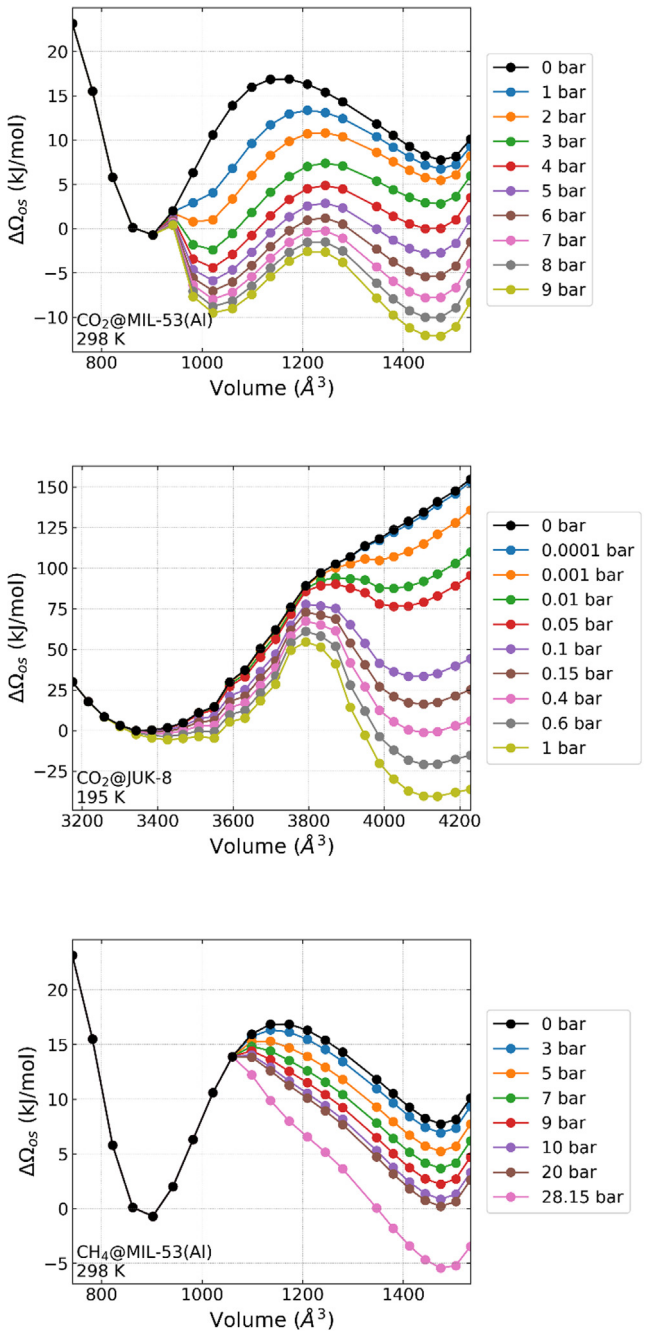

Fig. 6. Osmotic potential of CO_2 in MIL-53(Al) (298 K, top), CO_2 in JUK-8 (195 K, middle) and CH_4 in MIL-53(Al) (298 K, bottom). Full range of CO_2 gas pressures for JUK-8 is presented on Fig. S4.

one and corresponds to the *lp* structure. Therefore, the adsorption potential (Fig. 5, bottom panel) plays critical role in stabilization of *lp* phase, whereas the framework free energy restrains the structure from further expansion. The picture is totally different in the case of CO_2 adsorption, when both parts of osmotic potential contribute to produce a double-well energy landscape and causes breathing-like transformation of the framework.

The osmotic potential for adsorption of CO_2 in JUK-8 shows two minima, corresponding to *cp* and *op* phases, and indicates that the transitions between them is possible. For pressures up to 0.004 bar only one significant minimum of Ω_{os} exists; it corresponds to the *cp* phase, stabilized by the free energy of the framework. When the gas pressure increases to 0.05 bar, a shallow minimum appears at around 4050 Å^3 (the volume corresponding the *op* phase). In the range of pressure from 0.1 bar to 1 bar the *op* structure rapidly stabilizes; the equilibrium between *cp* and *op* phases occurs at approx. 0.4 bar. This pressure is slightly overestimated with respect to the experimentally observed transition range, between 0.1 bar and 0.2 bar (Fig. 4, middle panel). The *op* phase minimum for pressures close to 1 bar is relatively flat and may explain structure swelling reported in Ref. [15]. The transition between *cp* and *op* structures occurs as a result of two competing factors - *cp* phase is stabilized by the free energy of the framework and *op* phase is stabilized by the guest-host interactions.

3.4. Prediction of adsorption isotherms and framework deformation. Adsorption stress model.

The minima of the osmotic potential allowed us to predict the theoretical, equilibrium adsorption isotherms in different structural conformations of MIL-53(Al). Fig. 7 (top panel) shows the calculated adsorption isotherms for CO_2 adsorption in *np* and *lp* phases of MIL-53 at 297 K. The pressure of equilibrium transition between the isotherms is defined as the one for which the osmotic potentials of *np* and *lp* phases are equal. Experimentally, the phase transitions in MOFs rarely occur at the equilibrium conditions; due to significant energy barriers in the structures a large hysteresis between the phases is rather observed. In the case of CO_2 adsorption on MIL-53(Cr) [27] the *np* → *lp* transition develops over a wide range of pressures (3 bar – 7 bar) [14]: it begins by a reversible elastic deformation of 2.7% – 3.6% of unit cell volume, followed by spontaneous plastic transformation of the whole sample, involving up to 42% change of its volume.

To analyze the variation of mechanical properties of MIL-53(Al) upon CO_2 adsorption, we calculated the adsorption stress (Equations 8–10). For that we needed to estimate Henry constant K_H, saturation capacity N_0 and their derivatives with respect to the variation of cell volume upon adsorption. Therefore, we first reconstructed the isotherms for *np* and *lp* phases. We assumed that the (constant) volumes of unit cells of phases are equal to volumes at which the osmotic potential reaches the minimum. As these volumes are almost independent on gas pressure (see Fig. 6, top panel), for simplicity in further calculations we used the structures' volumes observed at equilibrium between phases (at the pressure of 7 bar): 1022 Å^3 for *np* phase and 1474 Å^3 for *lp* phase, respectively. The equilibrium isotherms were fitted to Langmuir model $N = N_0 \frac{K_H p}{N_0 + K_H p}$, and the derivatives $\frac{dN_0}{dV_c}$ and $\frac{dK_H}{dV_c}$ were extracted from the volume dependency of the K_H and N_0 constants. All parameters necessary to calculate the adsorption stress are collected in Table 1. Adsorption stress σ_s for each phase was then calculated using Eq. (9), and its value was calibrated (by adding a constant) to set $\sigma_s = 0$ at equilibrium pressure $p = 7 bar$.

The bulk modulus K_B of the framework at T = 300 K was calculated as the second derivative of free energy (Fig. 8, right) at volumes for which it reaches minima (Fig. 8, left). The obtained values, $K_B = 3.6 GPa$ and $K_B = 2.6 GPa$ for *np* and *lp* phases, respectively, confirm that the closed pores *np* structure is stiffer than the open structure. This result is intuitive, as deformations of denser structure need larger energy expense.

Using the calculated values of framework bulk modulus and the adsorption stress, the effective deformation of the framework upon CO_2 adsorption was calculated as a function of pressure (see Equation (9)). Fig. 8 (bottom panel) shows the variation of unit cell volume as a function of gas pressure, for *np* and *lp* structures. At very low pressures, (up to approximately 0.2 bar) the *np* structure contracts first (due to strong electrostatic interactions between hydroxyl groups and adsorbed CO_2 molecules), then expands by approx. 2% to 1022 Å^3 as the pressure increases. At the equilibrium transition pressure (7 bar) the structural transition from *np* to *lp* phase

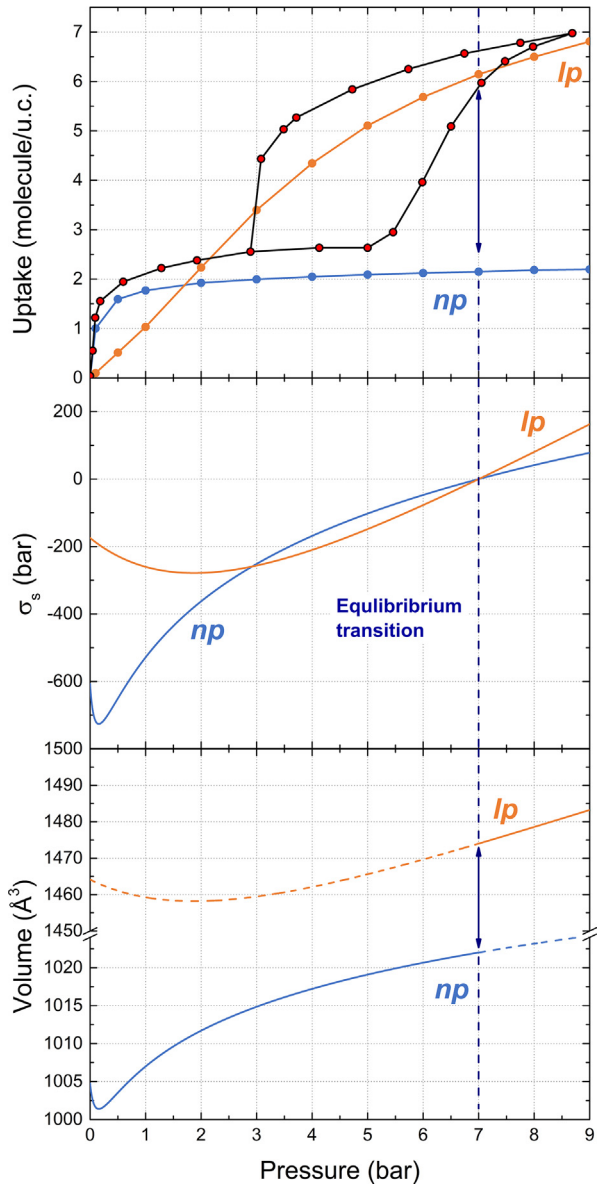

Fig. 7. Top: Isotherms of CO_2 adsorption in MIL-53(Al) at T = 297 K, reconstructed from osmotic free energy; middle: adsorption stress; bottom: volume of the unit cell for *np* and *lp* phases of MIL-53(Al).The dashed line indicates the equilibrium transition between phases, deduced from volume dependence of the osmotic potential (Fig. 6, top panel). Red points represent experimental data[15].

occurs, and the unit cell volume abruptly increases by 460 Å^3, reaching the value of 1483 Å^3 at 9 bar. This results agrees quantitatively with previously reported experimental observations [27].

The adsorption-induced deformations in JUK-8 will not be discussed here due to ambiguity in method of estimation of bulk modulus for *op* phase, for which minima of F_{host} does not exist. This aspect requires more deep insight and will be described in separate paper.

3.5. Modification of dispersion correction

The DFT methodology offers a vast selection of density functionals, starting from local-density approximation (LDA), through generalized-gradient approximation (GGA), up to hybrid functionals (e.g. B3LYP and metaGGA [49,50]), which can be applied to study a variety of material properties. However, many authors pointed out the difficulty of selecting the best functional to describe structural properties of MOFs: lattice constants, bond length, bond angles, and corresponding elastic constants. Nazarian *et al.* [51] performed a benchmarking study on a group of mostly non-porous, rigid MOFs with two GGA-type (PBE and PW91), one metaGGA (M06L), and tree dispersion corrected (PBE-D2, PBE-D3, and vdw-DF2) functionals. The authors showed that neither of generic functionals were able to properly describe all structures, and therefore the choice of the functional can be based on its availability in DFT code used, and on its computational robustness. We have tested [47] PBE and PBEsol functionals, with and without D2 and TS dispersion corrections on a set of flexible and rigid MOFs including MIL-53(Al) (*lp* and *np* phases), MIL-53(Sc) (*cp* phase) and MIL-53(Fe) (*int* phase). We have shown that although the dispersion correction tends to overestimate the long-range interactions, it is required to properly describe the contracted pore phases of studied materials. If the long-range interactions are neglected, the *np*, *cp*, and *int* phases in MIL-53 with different metals cannot be stabilized, and the optimization of framework geometry always ends up with open pore structure. The dispersion correction is then necessary to obtain double-well potential profile properly describing both phases in MIL-53 materials.

For MIL-53(Cr) Cockayne [52] showed that the difference of energy between *lp* and *np* phase (always more stable) varies in the range from 5 kJ/mol to 80 kJ/mol, depending on selected functional and dispersion correction. Similar problem was encountered by Hoffman *et al.* [33] when studying the energy profiles of MIL-53 (Al) using PBE-D3(BJ) functional: it was impossible to stabilize the *lp* structure at 300 K even when vibrational entropy was taken into account. The same conclusions were drown with a vast selection of the state-of-art dynamic methods [18].

Since the dispersion correction term is empirical and designed to fit a set of experimental data [45], the simplest modification of the PBE-D-type functionals that could improve the agreements between calculated and the experimentally observed phase diagram consists in rescaling of the dispersion term. Therefore we slightly reduced it, by 7% ($E_{el}(V) = E_{DFT}(V) + 0.93 \cdot E_{disp}(V)$). Corrected and uncorrected energy profiles are presented on Fig. 9 (free energy profile change with respect to scaling coefficient is presented on the Fig. S2). For MIL-53(Al) rescaling of the dispersion term stabilizes both *np* and *lp* phases at room temperature (T = 300 K), consistently with experimental data [53]. In the case of JUK-8 the influence of the rescaling of the dispersion correction on the free energy profile is much less significant and consists only in slight shift of the profile towards larger volumes.

Fig. 10 shows osmotic energy profiles calculated using corrected free energy contribution. For MIL-53(Al) the reduction of dispersion energy substantially improves the compliance of simulations

Table 1
Parameters used to calculate the adsorption stress for CO_2 adsorption in MIL-53(Al).

Phase	K_H	N_0	V_c	$\frac{dK_H}{dV_c}$	$\frac{dN_0}{dV_c}$
	(bar^{-1})	$(molecules/uc)$	$(Å^3)$	$(bar^{-1}Å^{-3})$	$(Å^{-3})$
lp	1.88	11.43	1021.62	$-3.4{\cdot}10^{-3}$	$4.6{\cdot}10^{-1}$
np	15.10	2.14	1474.35	$-6.4{\cdot}10^{-2}$	$4.9{\cdot}10^{-2}$

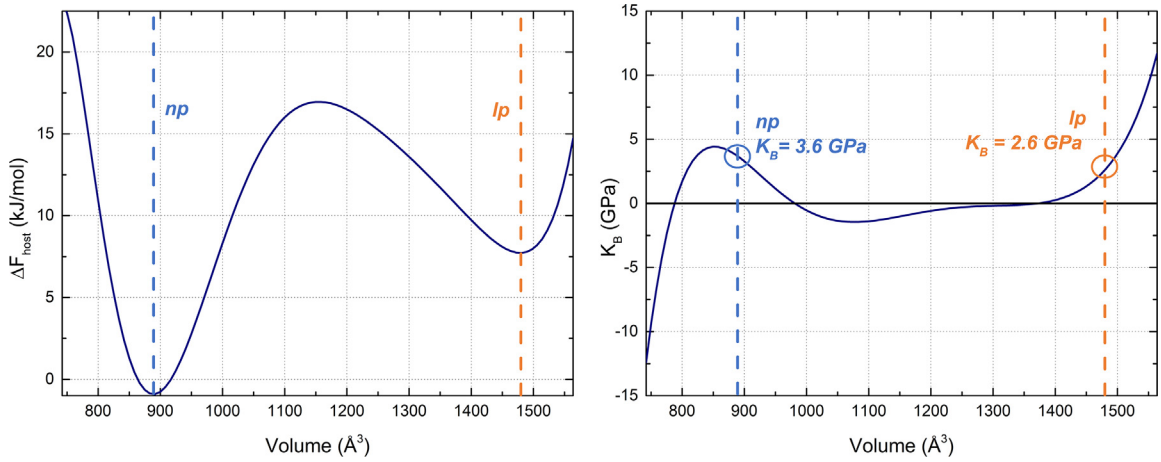

Fig. 8. Polynomial fit (9th) of free energy of MIL-53(Al) at 300 K (left) and its second derivative – bulk modulus (right), as a function of the unit cell volume.

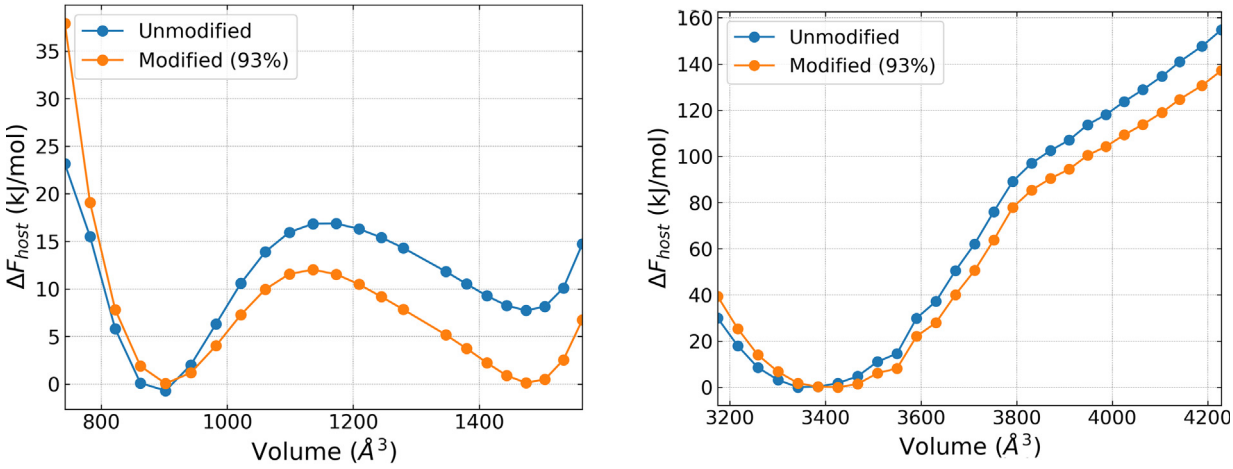

Fig. 9. Free energy for MIL-53(Al) (T = 300 K, left), and in for JUK-8 (T = 195 K, right). In blue: profiles calculated using unmodified dispersion correctional; in orange: with dispersion energy reduced by 7%.

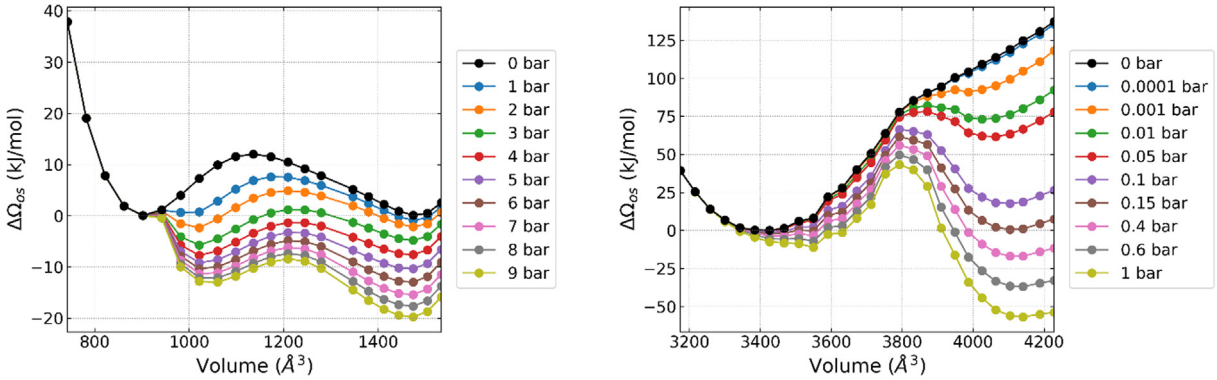

Fig. 10. Osmotic potential of CO_2 in MIL-53(Al) (left) and in JUK-8 (right) calculated with dispersion corrected free energies. Full range of CO_2 gas pressures for JUK-8 is presented on Fig. S5.

results with experimental data: the volumes for which the potential reaches minima remain almost unchanged, but the relative depth of the minima (relative stability of the np and lp phase) is different (compare to Fig. 6, top panel). The equilibrium transition is shifted towards lower gas pressures, to roughly 4 bar, which is within the range of experimentally observed hysteresis (Fig. 11). Similarly, for JUK-8 the transition is shifted to roughly 0.15 bar, the value which is much closer to experimentally observed value of 0.1 bar (Fig. 4). Therefore, the proposed rescaling of dispersion term provides satisfactory results for both studied materials; however, its universality have still to be tested on a significantly larger set of frameworks.

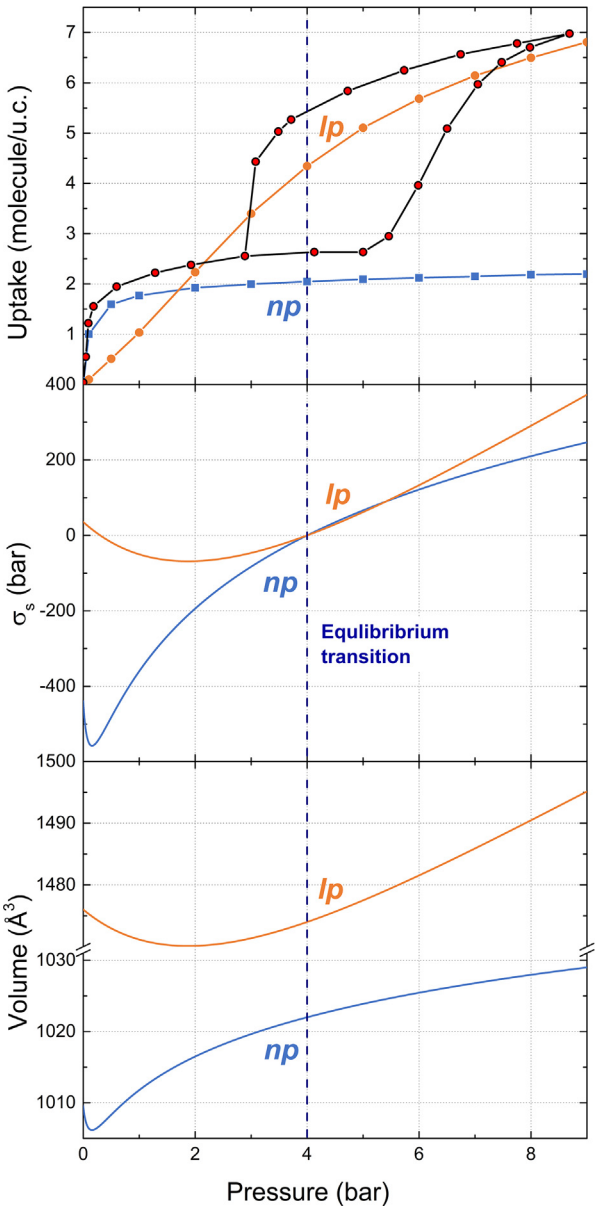

Fig. 11. Top: Isotherms of CO_2 adsorption in MIL-53(Al) at T = 297 K, reconstructed from the modified osmotic free energy (with rescaled dispersion term); middle: adsorption stress; bottom: volume of the unit cell for *np* and *lp* phases. The dashed line indicates the equilibrium transition between phases, deduced from volume dependence of the osmotic potential (Fig. 10, left panel). Red points represent experimental data [15].

4. Conclusions

We showed that a systematic use of the osmotic potential to characterize the adsorption-induced deformations in two MOFs – MIL-53(Al) and recently synthesized JUK-8 – gives the qualitative and quantitative description of the phenomena, in agreement with experimental results. The osmotic potential takes into account both factors involved in framework deformation: (i) the intrinsic capacity of the dry (empty) structure to deform, described by deformation energy terms (including the temperature-dependent lattice vibrations), and (ii) the adsorption stress, exerted by the adsorbed phase. Both components can be determined numerically by combining the electronic DFT and GCMC simulations for calculating respectively the energy of deformation, and adsorption isotherms. It is important to highlight that the approach we propose does not refer to neither arbitrary assumptions nor empirical (adjustable) parameters. We proved that the adsorption-induced transformations can be predicted without any experimental input. Therefore, the analysis of the osmotic thermodynamic potential provides a justified numerical alternative to the experimental investigations and should be applied as the first-step, rapid method of predicting, analyzing, and interpreting various forms of flexibility in MOF materials. The proposed approach can be applied to any flexible material which undergoes complex transformations through intermediate deformed phase. It can also be used to describe frameworks from DUT family, which exhibit NGA.

We also pointed out the critical importance of the dispersion contribution into interaction potentials in quantitative analysis of structural transformations of flexible structures. The fact that the reduction of the dispersion contribution by few percent only may change the shape of the framework free energy landscape and shift the conditions of phase stability was unexpected. It suggests that the dispersion term plays much more important role in the description of interactions than the thermodynamic correction of potentials for the vibrational anharmonicity evoked in earlier reports [18]. However, this conclusion needs to be further tested for a significantly larger set of frameworks in order to prove its importance.

CRediT authorship contribution statement

Filip Formalik: Conceptualization, Methodology, Validation, Formal analysis, Investigation, Writing - original draft, Writing - review & editing, Visualization, Funding acquisition. **Alexander V. Neimark:** Conceptualization, Methodology, Writing - review & editing, Supervision. **Justyna Rogacka:** Investigation, Visualization. **Lucyna Firlej:** Investigation, Writing - review & editing, Supervision. **Bogdan Kuchta:** Conceptualization, Formal analysis, Investigation, Writing - review & editing, Supervision, Project administration, Funding acquisition.

Declaration of Competing Interest

The authors declare that they have no known competing financial interests or personal relationships that could have appeared to influence the work reported in this paper.

Acknowledgments

F.F. is supported by the Polish National Science Centre (NCN, Grant ETIUDA No. 2018/28/T/ST4/00234. B.K. and J.R. are supported by the Polish national Science Centre (NCN, Grant OPUS No. 2015/17/B/ST8/00099). A.V.N. is supported by the National Science Foundation (CBET grant No. 1834339). This research was supported in part by PL-Grid Infrastructure.

Appendix A. Supplementary data

Supplementary data to this article can be found online at https://doi.org/10.1016/j.jcis.2020.05.105.

References

[1] A. Schneemann, V. Bon, I. Schwedler, I. Senkovska, S. Kaskel, R.A. Fischer, Flexible metal-organic frameworks, Chem. Soc. Rev. 43 (2014) 6062–6096, https://doi.org/10.1039/c4cs00101j.
[2] S. Krause, V. Bon, I. Senkovska, U. Stoeck, D. Wallacher, D.M. Többens, S. Zander, R.S. Pillai, G. Maurin, F.X. Coudert, S. Kaskel, A pressure-amplifying framework material with negative gas adsorption transitions, Nature. 532 (2016) 348–352, https://doi.org/10.1038/nature17430.
[3] J. Rogacka, F. Formalik, A.L. Triguero, L. Firlej, B. Kuchta, S. Calero, Intermediate states approach for adsorption studies in flexible metal-organic frameworks,

Phys. Chem. Chem. Phys. 21 (2019) 3294–3303, https://doi.org/10.1039/c8cp06817h.
[4] S.M.J. Rogge, M. Waroquier, V. Van Speybroeck, Unraveling the thermodynamic criteria for size- dependent spontaneous phase separation in soft porous crystals, Nat. Commun. 10 (2019) 4842, https://doi.org/10.1021/ba-1973-0121.ch001.
[5] F. Millange, C. Serre, G. Férey, Synthesis, structure determination and properties of MIL-53as and MIL-53ht: the first CrIII hybrid inorganic–organic microporous solids: CrIII(OH)·{O2C–C6H4–CO2}·{HO2C–C6H4–CO2H}x, Chem. Commun. 822–823 (2002).
[6] C. Serre, F. Millange, C. Thouvenot, M. Noguès, G. Marsolier, D. Louër, G. Férey, Very large breathing effect in the first nanoporous chromium(III)-based solids: MIL-53 or CrIII(OH)·{O2C-C6H4- CO2}·{HO2C-C6H4 -CO2H}x·H2Oy, J. Am. Chem. Soc. 124 (2002) 13519–13526, https://doi.org/10.1021/ja0276974.
[7] P.L. Llewellyn, G. Maurin, T. Devic, S. Loera-Serna, N. Rosenbach, C. Serre, S. Bourrelly, P. Horcajada, Y. Filinchuk, G. Férey, Prediction of the conditions for breathing of metal organic framework materials using a combination of X-ray powder diffraction, microcalorimetry, and molecular simulation, J. Am. Chem. Soc. 130 (2008) 12808–12814, https://doi.org/10.1021/ja803899q.
[8] G. Férey, C. Serre, Large breathing effects in three-dimensional porous hybrid matter: Facts, analyses, rules and consequences, Chem. Soc. Rev. 38 (2009) 1380–1399, https://doi.org/10.1039/b804302g.
[9] D. Fairen-Jimenez, S.A. Moggach, M.T. Wharmby, P.A. Wright, S. Parsons, T. Düren, Opening the gate: Framework flexibility in ZIF-8 explored by experiments and simulations, J. Am. Chem. Soc. 133 (2011) 8900–8902, https://doi.org/10.1021/ja202154j.
[10] A. Ghoufi, A. Subercaze, Q. Ma, P.G. Yot, Y. Ke, I. Puente-Orench, T. Devic, V. Guillerm, C. Zhong, C. Serre, G. Férey, G. Maurin, Comparative guest, thermal, and mechanical breathing of the porous metal organic framework MIL-53(Cr): A computational exploration supported by experiments, J. Phys. Chem. C. 116 (2012) 13289–13295, https://doi.org/10.1021/jp303686m.
[11] Y. Liu, J. Her, A. Dailly, A.J. Ramirez-cuesta, Reversible Structural Transition in MIL-53 with Large Temperature Hysteresis, J. Am. Chem. Soc. 130 (2008) 11813–11818.
[12] A. Boutin, D. Bousquet, A.U. Ortiz, F.X. Coudert, A.H. Fuchs, A. Ballandras, G. Weber, I. Bezverkhyy, J.P. Bellat, G. Ortiz, G. Chaplais, J.L. Paillaud, C. Marichal, H. Nouali, J. Patarin, Temperature-induced structural transitions in the gallium-based MIL-53 metal-organic framework, J. Phys. Chem. C. 117 (2013) 8180–8188, https://doi.org/10.1021/jp312179e.
[13] R. Schmid, An Electric Field Induced Breath for Metal-Organic Frameworks, ACS Cent. Sci. 3 (2017) 369–371, https://doi.org/10.1021/acscentsci.7b00162.
[14] A. Boutin, A.V. Neimark, A.H. Fuchs, The Behavior of Flexible MIL-53(Al) upon CH4 and CO2 Adsorption, J. Phys. Chem. C. 114 (2010) 22237–22244.
[15] K. Roztocki, F. Formalik, A. Krawczuk, I. Senkovska, B. Kuchta, S. Kaskel, D. Matoga, Collective Breathing in an Eightfold Interpenetrated Metal-Organic Framework: From Mechanistic Understanding towards Threshold Sensing Architectures, Angew. Chemie. 132 (2020) 4521–4527, https://doi.org/10.1002/ange.201914198.
[16] A.S. Munn, A.J. Ramirez-Cuesta, F. Millange, R.I. Walton, Interaction of methanol with the flexible metal-organic framework MIL-53(Fe) observed by inelastic neutron scattering, Chem. Phys. 427 (2013) 30–37, https://doi.org/10.1016/j.chemphys.2013.05.017.
[17] L. Chen, J.P.S. Mowat, D. Fairen-Jimenez, C.A. Morrison, S.P. Thompson, P.A. Wright, T. Düren, Elucidating the breathing of the metal-organic framework MIL-53(Sc) with ab initio molecular dynamics simulations and in situ X-ray Powder Diffraction Experiments, J. Am. Chem. Soc. 135 (2013) 15763–15773, https://doi.org/10.1021/ja403453g.
[18] R. Demuynck, S.M.J. Rogge, L. Vanduyfhuys, J. Wieme, M. Waroquier, V. Van Speybroeck, Efficient Construction of Free Energy Profiles of Breathing Metal-Organic Frameworks Using Advanced Molecular Dynamics Simulations, J. Chem. Theory Comput. 13 (2017) 5861–5873, https://doi.org/10.1021/acs.jctc.7b01014.
[19] N.A. Ramsahye, G. Maurin, S. Bourrelly, P.L. Llewellyn, T. Loiseau, C. Serre, G. Férey, On the breathing effect of a metal-organic framework upon CO2 adsorption: Monte Carlo compared to microcalorimetry experiments, Chem. Commun. (2007) 3261–3263, https://doi.org/10.1039/b702986a.
[20] F. Salles, A. Ghoufi, G. Maurin, R.G. Bell, C. Mellot-Draznieks, G. Férey, Molecular dynamics simulations of breathing MOFs: Structural transformations of MIL-53(Cr) upon thermal activation and CO2 adsorption, Angew. Chemie - Int. Ed. 47 (2008) 8487–8491, https://doi.org/10.1002/anie.200803067.
[21] F. Millange, N. Guillou, R.I. Walton, J.M. Grenèche, I. Margiolaki, G. Férey, Effect of the nature of the metal on the breathing steps in MOFs with dynamic frameworks, Chem. Commun. (2008) 4732–4734, https://doi.org/10.1039/b809419e.
[22] A. Boutin, M.A. Springuel-Huet, A. Nossov, A. Gédéon, T. Loiseau, C. Volkringer, G. Férey, F.X. Coudert, A.H. Fuchs, Breathing transitions in MIL-53(A1) metal-organic framework upon Xenon adsorption, Angew. Chemie - Int. Ed. 48 (2009) 8314–8317, https://doi.org/10.1002/anie.200903153.
[23] A. Ghoufi, G. Maurin, G. Férey, Physics behind the guest-assisted structural transitions of a porous metal-organic framework material, J. Phys. Chem. Lett. 1 (2010) 2810–2815, https://doi.org/10.1021/jz1011274.
[24] F.-X. Coudert, M. Jeffroy, A.H. Fuchs, A. Boutin, C. Mellot-Draznieks, Thermodynamics of Guest-Induced Structural Transitions in Hybrid Organic - Inorganic Frameworks, J. Am. Chem. Soc. 130 (2008) 14294–14302.
[25] F.X. Coudert, The osmotic framework adsorbed solution theory: Predicting mixture coadsorption in flexible nanoporous materials, Phys. Chem. Chem. Phys. 12 (2010) 10904–10913, https://doi.org/10.1039/c003434g.
[26] A.V. Neimark, F.X. Coudert, A. Boutin, A.H. Fuchs, Stress-based model for the breathing of metal-organic frameworks, J. Phys. Chem. Lett. 1 (2010) 445–449, https://doi.org/10.1021/jz9003087.
[27] A.V. Neimark, F.X. Coudert, C. Triguero, A. Boutin, A.H. Fuchs, I. Beurroies, R. Denoyel, Structural transitions in MIL-53 (Cr): View from outside and inside, Langmuir. 27 (2011) 4734–4741, https://doi.org/10.1021/la200094x.
[28] C. Triguero, F.X. Coudert, A. Boutin, A.H. Fuchs, A.V. Neimark, Mechanism of breathing transitions in metal-organic frameworks, J. Phys. Chem. Lett. 2 (2011) 2033–2037, https://doi.org/10.1021/jz2008769.
[29] F.X. Coudert, A. Boutin, A.H. Fuchs, A.V. Neimark, Adsorption deformation and structural transitions in metal-organic frameworks: From the unit cell to the crystal, J. Phys. Chem. Lett. 4 (2013) 3198–3205, https://doi.org/10.1021/jz4013849.
[30] A. Ghysels, L. Vanduyfhuys, M. Vandichel, M. Waroquier, V. Van Speybroeck, B. Smit, On the Thermodynamics of Framework Breathing: A Free Energy Model for Gas Adsorption in MIL-53, J. Phys. Chem. C. 117 (2013) 11540–11554, https://doi.org/10.1021/jp311601q.
[31] L. Vanduyfhuys, S.M.J. Rogge, J. Wieme, S. Vandenbrande, G. Maurin, M. Waroquier, V. Van Speybroeck, Thermodynamic insight into stimuli-responsive behaviour of soft porous crystals, Nat. Commun. 9 (2018) 1–9, https://doi.org/10.1038/s41467-017-02666-y.
[32] A.E.J. Hoffman, L. Vanduyfhuys, I. Nevjestić, J. Wieme, S.M.J. Rogge, H. Depauw, P. Van Der Voort, H. Vrielinck, V. Van Speybroeck, Elucidating the Vibrational Fingerprint of the Flexible Metal-Organic Framework MIL-53(Al) Using a Combined Experimental/Computational Approach, J. Phys. Chem. C. 122 (2018) 2734–2746, https://doi.org/10.1021/acs.jpcc.7b11031.
[33] A.E.J. Hoffman, J. Wieme, S.M.J. Rogge, L. Vanduyfhuys, V. Van Speybroeck, The impact of lattice vibrations on the macroscopic breathing behavior of MIL-53 (Al), Zeitschrift Fur Krist. - Cryst. Mater. 234 (2019) 529–545, https://doi.org/10.1515/zkri-2018-2154.
[34] D. Li, K. Kaneko, Hydrogen bond-regulated microporous nature of copper complex-assembled microcrystals, Chem. Phys. Lett. 335 (2001) 50–56, https://doi.org/10.1016/S0009-2614(00)01419-6.
[35] B. Chen, C. Liang, J. Yang, D.S. Contreras, Y.L. Clancy, E.B. Lobkovsky, O.M. Yaghi, S. Dai, A microporous metal-organic framework for gas-chromatographic separation of alkanes, Angew. Chemie - Int. Ed. 45 (2006) 1390–1393, https://doi.org/10.1002/anie.200502844.
[36] C.O. Ania, E. García-Pérez, M. Haro, J.J. Gutiérrez-Sevillano, T. Valdés-Solís, J.B. Parra, S. Calero, Understanding gas-induced structural deformation of ZIF-8, J. Phys. Chem. Lett. 3 (2012) 1159–1164, https://doi.org/10.1021/jz300292y.
[37] N.Y. Tan, M.T. Ruggiero, C. Orellana-Tavra, T. Tian, A.D. Bond, T.M. Korter, D. Fairen-Jimenez, J. Axel Zeitler, Investigation of the terahertz vibrational modes of ZIF-8 and ZIF-90 with terahertz time-domain spectroscopy, Chem. Commun. 51 (2015) 16037–16040, https://doi.org/10.1039/c5cc06455d.
[38] M.R. Ryder, B. Civalleri, T. Bennett, S. Henke, S. Rudić, G. Cinque, F. Fernandez-Alonso, J.C. Tan, Identifying the role of terahertz vibrations in metal-organic frameworks: From gate-opening phenomenon to shear-driven structural destabilization, Phys. Rev. Lett. 113 (2014) 1–6, https://doi.org/10.1103/PhysRevLett.113.215502.
[39] F. Formalik, M. Fischer, J. Rogacka, L. Firlej, B. Kuchta, Effect of low frequency phonons on structural properties of ZIFs with SOD topology, Microporous Mesoporous Mater. 109132 (2018), https://doi.org/10.1016/j.micromeso.2018.09.033.
[40] J.D. Evans, L. Bocquet, F.X. Coudert, Origins of Negative Gas Adsorption, Chem. 1 (2016) 873–886, https://doi.org/10.1016/j.chempr.2016.11.004.
[41] S. Krause, J.D. Evans, V. Bon, I. Senkovska, S. Ehrling, U. Stoeck, P.G. Yot, P. Iacomi, P. Llewellyn, G. Maurin, F.X. Coudert, S. Kaskel, Adsorption Contraction Mechanics: Understanding Breathing Energetics in Isoreticular Metal-Organic Frameworks, J. Phys. Chem. C. 122 (2018) 19171–19179, https://doi.org/10.1021/acs.jpcc.8b04549.
[42] G. Kresse, J. Furthmuller, Efficiency of ab-initio total energy calculations for metals and semiconductors using a plane-wave basis set, Comput. Mater. Sci. 6 (1996) 15–50, https://doi.org/10.1016/0927-0256(96)00008-0.
[43] G. Kresse, J. Furthmuller, Efficient iterative schemes for ab initio total-energy calculations using a plane-wave basis set, Phys. Rev. B. 54 (1996) 11169–11186, https://doi.org/10.1103/PhysRevB.54.11169.
[44] G. Kresse, J. Hafner, Ab initio molecular dynamics for liquid metals, Phys. Rev. B. 47 (1993) 558–561, https://doi.org/10.1103/PhysRevB.47.558.
[45] S. Grimme, Semiempirical GGA-Type Density Functional Constructed with a Long-Range Dispersion Correction, J. Comput. Chem. 27 (2006) 1787–1799, https://doi.org/10.1002/jcc.
[46] S. Grimme, S. Ehrlich, L. Goerigk, Effect of the Damping Function in Dispersion Corrected Density Functional Theory, J. Compuational Chem. 32 (2011) 1456–1465.
[47] F. Formalik, M. Fischer, J. Rogacka, L. Firlej, B. Kuchta, Benchmarking of GGA density functionals for modeling structures of nanoporous, rigid and flexible MOFs, J. Chem. Phys. 149 (2018), https://doi.org/10.1063/1.5030493 064110.
[48] P.I. Ravikovitch, A.V. Neimark, Density functional theory model of adsorption deformation, Langmuir. 22 (2006) 10864–10868, https://doi.org/10.1021/la061092u.
[49] J. Sun, M. Marsman, G.I. Csonka, A. Ruzsinszky, P. Hao, Y.S. Kim, G. Kresse, J.P. Perdew, Self-consistent meta-generalized gradient approximation within the

projector-augmented-wave method, Phys. Rev. B. 84 (2011) 1–12, https://doi.org/10.1103/PhysRevB.84.035117.
[50] J. Sun, A. Ruzsinszky, J. Perdew, Strongly Constrained and Appropriately Normed Semilocal Density Functional, Phys. Rev. Lett. 115 (2015) 1–6, https://doi.org/10.1103/PhysRevLett.115.036402.
[51] D. Nazarian, P. Ganesh, D.S. Sholl, Benchmarking density functional theory predictions of framework structures and properties in a chemically diverse test set of metal-organic frameworks, J. Mater. Chem. A. 3 (2015) 22432–22440, https://doi.org/10.1039/c5ta03864b.
[52] E. Cockayne, Thermodynamics of the Flexible Metal – Organic Framework Material MIL-53(Cr) From First-Principles, J. Phys. Chem. C. 121 (2017) 4312–4317, https://doi.org/10.1021/acs.jpcc.6b11692.
[53] Y. Liu, J. Her, A. Dailly, A.J. Ramirez-cuesta, Reversible Structural Transition in MIL-53 with Large Temperature, Hysteresis (2008) 11813–11818.